

# Discovery of ERBB3 inhibitors for non-small cell lung cancer (NSCLC) via virtual screening

Rong Guo<sup>1</sup> · Yuan Zhang<sup>1</sup> · Xiao Li<sup>1</sup> · Xinrui Song<sup>1</sup> · Da Li<sup>1</sup> · Yong Zhao<sup>1</sup>

Received: 17 February 2016 / Accepted: 2 May 2016  
© Springer-Verlag Berlin Heidelberg 2016

**Abstract** As a member of the epidermal growth factor receptor family (EGFR) of receptor tyrosine kinases, ERBB3 plays an important role in mediating cellular growth and differentiation. Recent research works identified that CD74-NRG1 fusions lead to overexpression of the EGF-like domain of NRG1, and thus activate ERBB3 and PI3K-AKT signaling pathways. The fusion was detected in lung adenocarcinomas, and served as an important oncogenic factor for ERBB3 driven cancers. A sequential virtual screening strategy has been applied to ERBB3 crystal structure using databases of natural products and Chinese traditional medicine compounds, and led to identification of a group of small molecular compounds potentially capable of blocking ERBB3. Six small molecular compounds were selected for in vitro analysis. Five of these molecules significantly inhibited the growth of A549 cells. Among them, compound VS1 is the most promising one with IC<sub>50</sub> values of 269.75 μM, comparing to the positive control of nimustine hydrochloride with IC<sub>50</sub> values of 264.14 μM. With good specificity and predicted ADMET results, our results support the feasibility by using a pharmacophore of the compound VS1 for designing and optimization of ERBB3 inhibitors.

**Keywords** ERBB3 · NRG1 · Virtual screening

## Introduction

As one of the most common malignant tumors around the world, lung cancer accounts for 1.8 million new cancer cases each year and claims 27 % of total cancer related death. Lung cancer is classified as non-small cell lung cancer (NSCLC) and small cell lung cancer (SCLC) according to the histological type. NSCLC makes up 80 % of all lung cancer cases and most of the patients are the elderly [1]. There are three subtypes of NSCLC, including adenocarcinoma (LUAD), squamous-cell carcinoma (LUSC), and large-cell carcinoma (LACC). Because of difficulties in early detection and diagnosis and tendency to metastasize, LUAD's 5-year survival rate is only about 15 % [2].

Significant advances in treatment of lung cancers have been achieved by targeting critical growth and survival pathways of cancer cells. Epidermal growth factor receptor (EGFR) is a transmembrane protein receptor with cytoplasmic kinase activity, responsible for transduction of extracellular growth and survival signals. More than 60 % of NSCLCs express EGFR and many of them contain somatic mutations leading to constitutive activation of EGFR signaling [3]. Recent clinical data showed that EGFR inhibitors were effective in treating the lung cancers with EGFR mutations [4]. EGFR is the prototypical member of the ERBB family of transmembrane receptor tyrosine kinases (RTK), which include ERBB1 (EGFR, HER1) [5], ERBB2 (HER2) [6], ERBB3 (HER3) [7], and ERBB4 (HER4) [8]. Deregulation of other members of ERBB receptors was also observed in human cancers, exemplified by overexpression of ERBB2 in many breast cancers. Inhibitors targeting EGFR and ERBB2 signaling have been developed successfully and used to treat lung and breast cancers.

ERBB family proteins exist in monomer in the absence of ligand binding, containing three regions: extracellular region,

✉ Yong Zhao  
zhaoyong@bcc.ac.cn

<sup>1</sup> Beijing Computing Center, NO.7 Fengxian Middle St, Haidian District, Beijing 100094, China

transmembrane region, and intracellular region. The extracellular region is responsible for ligand binding, and the intracellular region comprised of a typical ATP binding site, as well as the tyrosine kinase domain. Structural studies show that binding ligands of ERBBs promote the rearrangement of the extracellular region from a tethered to an extended conformation [9]. Through binding to the ligands, ERBBs form heterodimers or homodimers and induce the phosphorylation of the kinase domain, leading to the activation of the following PI3K-AKT and MAPK signaling pathways [10]. Among them, ERBB2 does not bind any known ERBB ligands and is activated via heterodimerization with other ligand bound ERBB proteins. ERBB3 has impaired kinase activity, only signaling through dimerization with ERBB proteins with active kinase activity, such as ERBB2.

The primary ligand for ERBB3 is neuregulin 1 (NRG1), a member of neuregulin family. NRG1 isoforms are mainly expressed in the nervous system, heart and breast, and all of them have an extracellular EGF-like domain, which can activate the heterodimerization of ERBB2-ERBB3 [11]. Recent genomic analysis identified some oncogene fusions as driver mutations in LUAD, including CD74-NRG1, SLC3A2-NRG1, EZR-ERBB4, TRIM24-BRAF, and KIAA-RET. [12] Among them, CD74-NRG1 fusion results in the overexpression of NRG1's extracellular EGF-like domain, which provides ligands for ERBB3 receptors, induces ERBB2-ERBB3 hetero-dimerization, and the subsequent activation of the PI3K-AKT and MAPK signaling pathways [13]. Therefore, inhibition of the activity of ERBB3 presents a desired strategy to treat LUAD caused by NRG1 fusions. Recent findings suggested ERBB3 is a promising drug target [14, 15], and its activation can be inhibited by directly blocking ligand-receptor interactions. Several ERBB3 inhibitors showing good pre-clinical results have been currently in different clinical phases, and are expected to be approved as potential innovative drugs. However, most of them are monoclonal antibodies [16–20], and the small molecular drugs are still under development.

Natural products contributed greatly to the new molecular entities (NMEs) in the history. Of all the FDA-approved NMEs introduced until now, roughly over one-third are natural products and their derivatives [21]. China has rich medicinal resources, where the well-known traditional Chinese medicine (TCM) has been practiced for more than 2000 years [22]. During the past few years, over 1000 plants were investigated and showed somewhat anticancer activities *in vivo*. Some biologically active natural products, including traditional Chinese medicine (TCM), would provide selective ligands for disease-related targets [23], influence or inhibit the disease-related pathways, and therefore provide potential lead compounds for the diseases. In this study, we reported an integrated computer aided approach searching for good

potential ERBB3 inhibitors among the known natural products or traditional Chinese medicine compounds.

We developed a computer-aided drug screening platform (<http://www.vslead.com>) to provide virtual screening, molecular dynamics simulation, and bioinformatics online services. To search for potential ERBB3 inhibitors, we used the sequential virtual screening workflow followed by cell based assay testing. Five novel inhibitors were identified as potential inhibitors of ERBB3 and could be further optimization as specific ERBB3 inhibitors.

## Experimental methods

### Databases construction

The structural information of natural products and traditional Chinese medicines was collected from both domestic and international mainstream databases, such as ZINC database. The format of compounds structures is converted to pdbqt format through Applied Chemistry Software openbabel [24]. To provide potential active compounds for the following structure-based virtual screening, we have successfully constructed a traditional Chinese medicines compounds database (TCMCD) containing 8445 kinds of active ingredients in traditional Chinese medicines and 33,765 molecular compounds, and a natural products database (NPD) containing 149,515 molecular compounds.

### Protein preparation and virtual screening

Computer-aided drug screening platform [25] is a platform for drug discovery, we use virtual screening module (<http://www.vslead.com/index.php?r=vina/index>) to carry out the virtual screening. Three aspects should be confirmed before submitting virtual screening tasks: compound database, prepared protein files, and the binding site of the target.

Crystal structure of ERBB3 was obtained from the Protein Data Bank (PDB code: 1M6B). Firstly, all water and solvent molecules were removed from the structure, hydrogen atoms and Gasteiger charges were added using AutoDock Tools [26], and the prepared protein file in pdbqt format was uploaded. Secondly, binding site should be identified and the relevant blanks need to be filled on the platform. Because of no complex structure of ERBB3, the grid-enclosing box was set to center on the β-hairpin cavity of domain II, which was thought to relate to the regulation of ligand binding. Center coordinate (center\_x: -1.51, center\_y: 45.26, center\_z : 55.24) and box size (size\_x: 20, size\_y: 18, size\_z: 20) of grid was proposed to enclose the whole β-hairpin cavity. Thirdly, NPD (~150 000 compounds) and TCMCD (~30 000 compounds) were selected and virtual screening task was submitted. Afterwards, the top 200 ranked compounds

from each database were selected for further visual inspection. Finally, binding affinity with the  $\beta$ -hairpin region and druggability were considered to select candidates. Compounds shape or molecular electrostatic potential matching with the active site of target would be selected, and more hydrogen bond interactions with residues (242–259) of the  $\beta$ -hairpin region would be added extra points. On the other hand, trade-off analysis of polar ring and non-polar group was proposed to consider druggability. As a result, 14 candidates from NPD and 13 candidates from TCMCD were selected.

### ADMET prediction

The failure of many drug candidates during clinical trials can be attributed to poor ADMET (absorption, distribution, metabolism, excretion, and toxicity) properties. However, the experimental evaluation of pharmacodynamics and toxicity profiles is costly and the workload is heavy, therefore, computational techniques that can filter/predict pharmacodynamics and toxicity profiles have become an alternative approach. Nowadays, computational approaches are used to assess the ADMET properties of compounds at the early stages of drug discovery and development. Here, we evaluated the ADMET properties of compounds using AdmetSAR [27] and pkCSM tools [28]. AdmetSAR and pkCSM are advanced computer programs that enable researchers to rapidly predict a large number of ADMET properties from a molecular structure. They have been considered widely as useful tools to predict physico-chemical and biological properties of drug-like chemicals [29–31].

### Chemistry

All compounds were purchased from two commercial suppliers, Yuanye ([www.shyuanye.com](http://www.shyuanye.com)) and Topscience ([www.tsbiochem.com](http://www.tsbiochem.com)), without further purification. HPLC analysis of these compounds confirmed that the purity was  $\geq 98\%$ .

### In vitro antiproliferation assay on A549 and MRC-5 cell lines

Cell viability was measured by the CCK-8 assay as previously described [32, 33]. Briefly, A549 cells and MRC-5 cells were plated into 96-well plates with 200  $\mu$ l of DMEM medium containing 10 % fetal bovine serum (FBS) and 1 % Penicillin-Streptomycin solution (PS) at a density of  $5 \times 10^4$  cells/well. We got six compounds solution at the concentration of 1 mg/ml by dissolving with 50 % DMSO. The cells were incubated with these six compounds, as well as the positive control nimustine hydrochloride, at different concentrations (1 mg/ml, 200  $\mu$ g/ml, 40  $\mu$ g/ml, 8  $\mu$ g/ml, 160 ng/ml, and 32 ng/ml) in a humidified incubator with 5 % CO<sub>2</sub>, 37 °C for

48 h. The cells were only incubated with DMSO at different concentrations (40 %, 8 %, 1.6 %, 0.32 %, 0.064 %, and 0.0128 %) in the negative control. At the end of each treatment, we discarded the supernatant and re-added 200  $\mu$ l of DMEM medium with 10 % FBS and 1 % PS; 20  $\mu$ l Cell Counting Kit-8 (CCK-8) was added to each well and cells were further cultured for 4 h. The absorbance was measured at a wavelength of 450 nm with a Synergy 2 multimode microplate reader (BioTek). The inhibition rate (%) was calculated by the formula:

$$\text{Inhibition\%} = \left( 1 - \frac{F_{450,\text{compound}}}{F_{450,\text{control}}} \right) \times 100\%$$

$IC_{50}$  values were calculated from the inhibition curves.

### Results and discussion

The structure of ERBB3 extracellular region is shown as Fig. 1. Domains I and III exhibit  $\beta$ -helical structure, and domains II and IV show extend rod-like structures with repeats of small disulfide-bonded modules [10]. As reported, the region between domain I and III is the ligand binding site. Residues Tyr246, Phe251, and Gln252 of  $\beta$ -hairpin loop (domain II, residues 242 to 259) contact the COOH-terminal of domain IV to create intramolecular interaction, which is important to keep ERBB3 in the ligand-free inactive conformation and sets a barrier to conformation rearrangement of ligand binding. The structural information of ERBB3 with ligands demonstrates a large conformation change and domain rearrangement occurring upon ligand binding, which breaks up domain II/IV intramolecular interaction and exposes the dimerization site in domain II for subsequent receptor dimerization and activation.

Actually, domain II/IV contact region is predicted as a potential pocket by PocketPicker23 [34] and antibody binding on it to trap ERBB3 in the tethered conformation has been proved feasible [35]. LJM716, a human monoclonal antibody currently in phase 1 clinical development, can inhibit ERBB3 in the tethered conformation through binding to an epitope within domain II and IV [35]. This provides us a rational approach to modulate the activation of ERBB3 by designing compounds binding to domain II/IV tethered region (the  $\beta$ -hairpin loop of domain II, domain II/IV contact region or the pocket of domain IV).

We select the cavity above the  $\beta$ -hairpin loop (Fig. 1c) for virtual screening, to search for small molecular inhibitors of the ERBB3 receptor. The inhibitors can suppress the NRGs-ERBB3 signal conduction process by blocking conformation rearrangement and keeping ERBB3 in an inactive state.

Virtual screening of natural products database (NPD) and traditional Chinese medicines compounds database

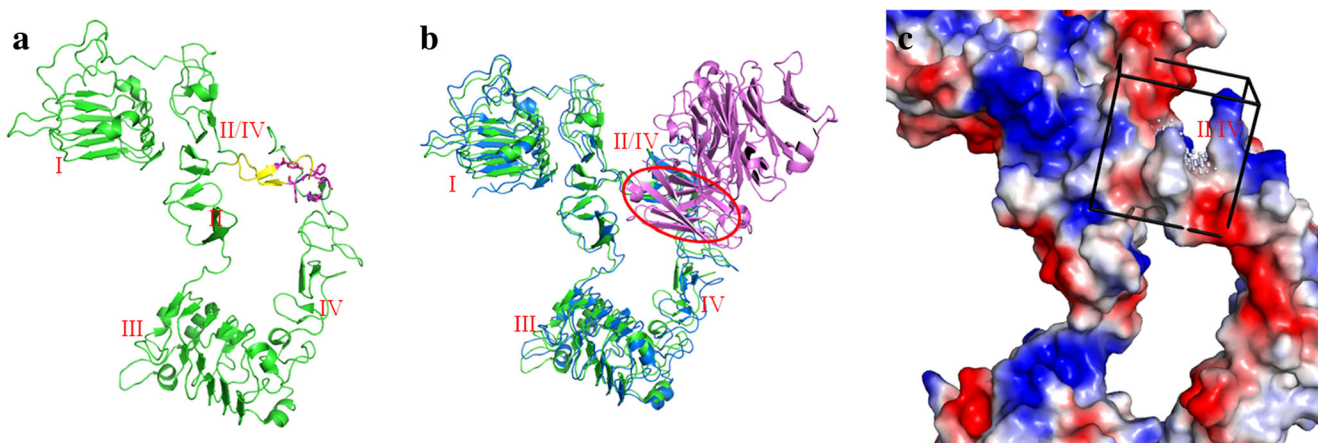


**Fig. 1** The crystal structure of the extracellular region of ERBB3. **a**) Ribbon representation of the ERBB3 extracellular region (PDB code: 1M6B). Four domains (I, II, III, and IV) are labeled in green,  $\beta$ -hairpin loop is colored yellow, while II/IV contact residues (Tyr246, Phe251, and Gln252) are colored magenta and shown in stick representation; **b**)

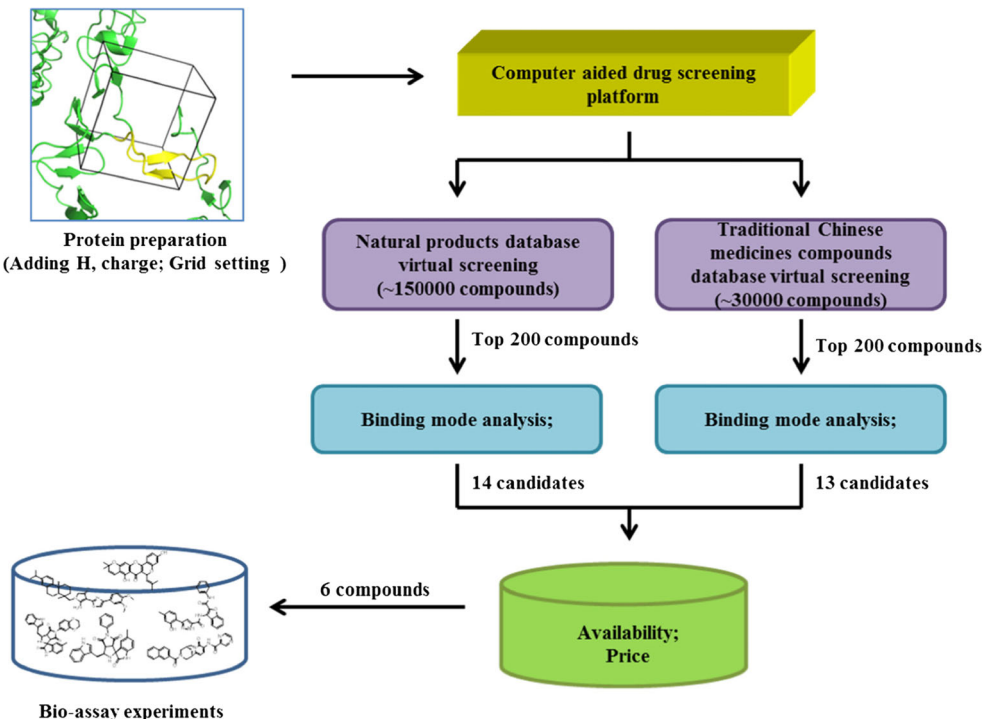
complex of ERBB3 (dark blue) and MOR09825 (purple) (PDB code: 4P59), MOR09825 is the parent Fab molecule of ERBB3 monoclonal antibody LJM716 [35]; **c**) Surface representation of ERBB3, active site used in virtual screening is indicated in black box, binding site predicted by PocketPicker plugin in Pymol is shown as gray spheres

(TCMCD) were performed on our computer-aided drug screening platform [36] (Fig. 2). First of all, the top 200 compounds ranked by binding free energy were selected for further structural analysis. Next, we manually checked the interaction models of these compounds with the  $\beta$ -hairpin region to remove the false positive results. Compounds that shape or molecular electrostatic potential matching with the  $\beta$ -hairpin region were selected. In addition, several in silico properties (AlogP, rotatable bond) were also considered in the screening process. Then, 14 candidates from NPD and 13 candidates from TCMCD were selected to consider for assay testing.

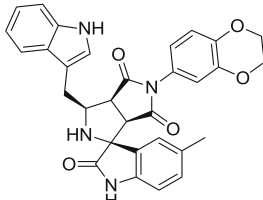
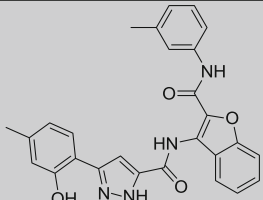
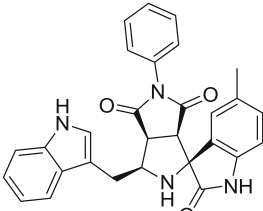
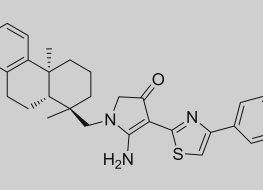
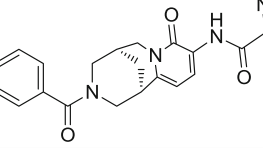
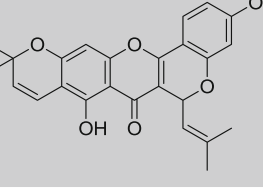
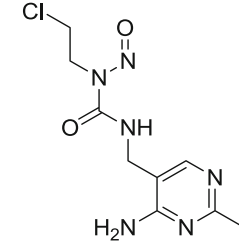
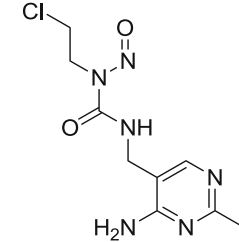
After checking the availability and prices provided by different suppliers, finally, six compounds (compounds VS1, VS2, VS3, VS4, VS5, and VS6) were purchased for further bioassay experiments.

To investigate whether the compounds actively inhibit NSCLC cell proliferation, six compounds (VS1, VS2, VS3, VS4, VS5, and VS6) were chosen for antiproliferation assay on A549 (human lung adenocarcinoma epithelial cells) and MRC-5 cell lines (human lung normal cells). Nimustine hydrochloride [37], an approved nitrosourea-derived anticancer agent effective against lung cancer [38], was selected to be the

**Fig. 2** Schematic representation of virtual screening on ERBB3 receptor



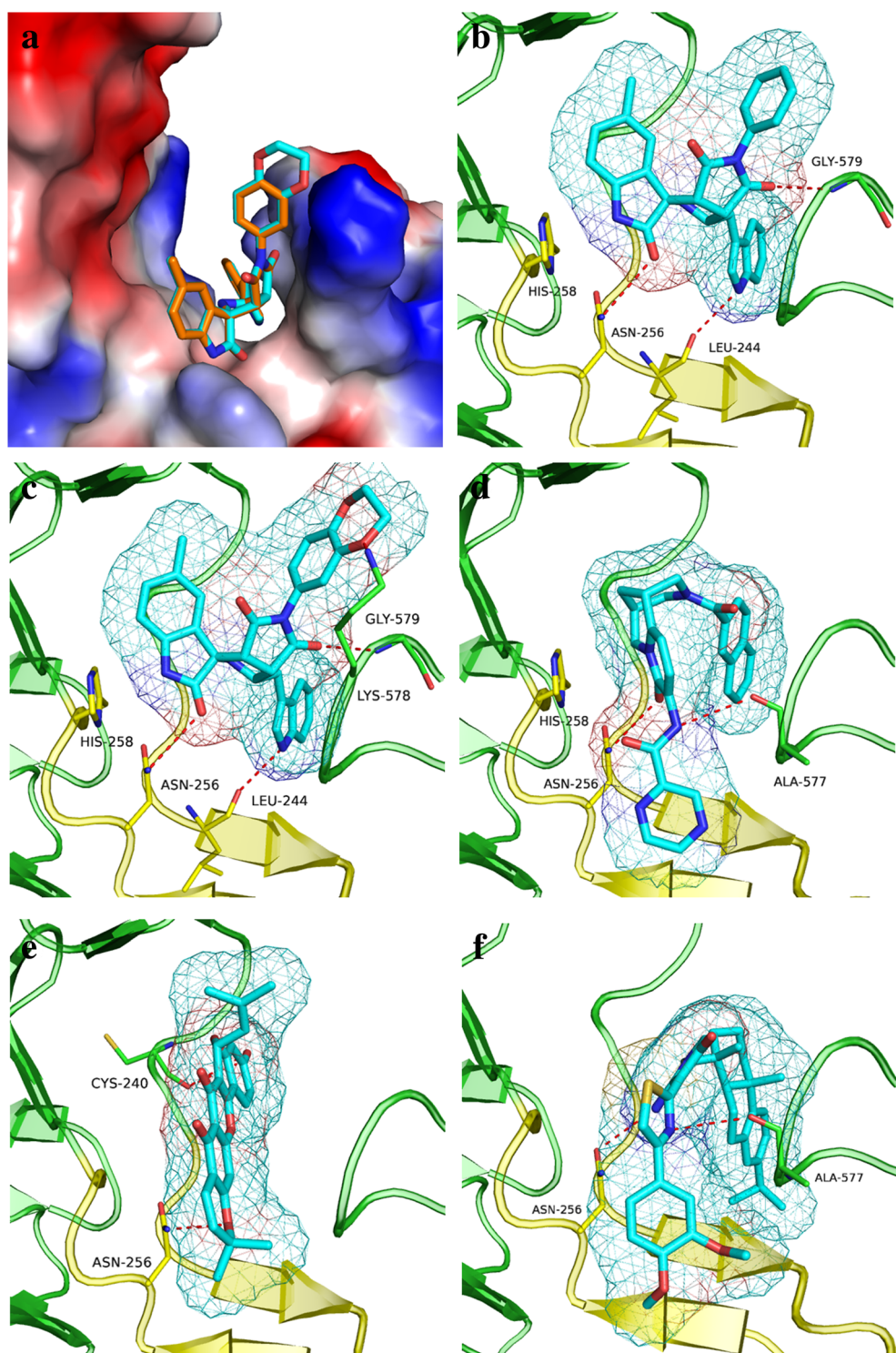
**Table 1** Structures and bioassay data of the compounds

Compound	Structure	A549 Cell line <sup>a</sup>	MRC-5 Cell line <sup>b</sup>
		IC <sub>50</sub> (μ M)	IC <sub>50</sub> (μ M)
<b>VS1</b>		269.75	305.14
<b>VS2</b>		1162.71	737.52
<b>VS3</b>		150.48	119.66
<b>VS4</b>		612.34	369.37
<b>VS5</b>		540.63	466.30
<b>VS6</b>		541.54	330.92
<b>Nimustine</b>		264.14	436.94
<b>Hydrochloride</b>			

<sup>a</sup> A549 cells are human lung adenocarcinoma epithelial cells<sup>b</sup> MRC-5 cells are human lung normal cells

positive control. The cells were incubated with various compounds at different concentrations for 48 h, and five of them, compounds VS1, VS3, VS4, VS5, and VS6, significantly inhibited the growth of A549 cells with  $IC_{50}$  values ranging from 150.48  $\mu\text{M}$  to 612.34  $\mu\text{M}$  (Table 1). As shown in Table 1, compound VS1 expresses good selectivity as its  $IC_{50}$  value of A549 cell line is much lower than that of

**Fig. 3** Predicted binding modes of compounds VS3(b), VS1(c), VS5(d), VS6(e), VS4(f) in the  $\beta$ -hairpin cavity of ERBB3 (PDB code: 1M6B). ERBB3 is colored in green, while  $\beta$ -hairpin loop is yellow, relevant residues are shown as sticks and labeled. Compounds are represented as cyan sticks. Potential hydrogen bond interactions are shown in red. Electrostatic potential diagram of ERBB3 with compound VS3 (colored in orange) and VS1 (colored in cyan) is shown in Fig. 3a



MRC-5 cell line. Thus five hits (compounds VS1, VS3, VS4, VS5, and VS6) were identified as novel inhibitors for ERBB3.

The potential binding modes of the five hits revealed by docking study are shown in Fig. 3. All of the five hits have aromatic rings to form van der Waals interaction with the  $\beta$ -hairpin region. In addition, all of them contain groups creating

several hydrogen bonds with  $\beta$ -hairpin's residues. Notably, they all have hydrogen bond interaction with residue Asn256, which might be a key residue for small molecular binding, and pi-pi interaction with residue His258 could be observed in compounds VS3, VS1, and VS5.

Among them, compounds VS3 and VS1 have the highest activity. Based on the docked conformation of compounds VS1 and VS3, a binding mode was proposed. Indole ring creates hydrophobic interactions with the non-polar pocket. The linker pyrrolidine ring fits the  $\beta$ -hairpin region through van der Waals interaction, the lactam ring interacts with residue His258 by weak pi-pi interaction, and the oxygen of carbonyl creates a hydrogen bond with the amino of amide in residue Asn256. The oxygen of carbonyl in the pyrrole ring interacts with the hydrogen of the main chain in residue Cly579 through hydrogen bond interaction, and the amide in the indole ring forms hydrogen bonds with residue Leu244. In addition, the only difference between compounds VS3 and VS1 is the oxygen-containing six-membered heterocycle. The oxygen of compound VS1 creates a hydrogen bond with the hydrogen of the amino in residue Lys578. However, the activity of compound VS3 is twice that of compound VS1, which may be because the hydrogen bond interaction with residue Lys578 is not the key interaction, or related to compound's dynamics inside the cell.

Interacting with residues through two hydrogen bonds, compounds VS4, VS5, and VS6 have moderate activity. The hydrogen bond interaction with residue Asn256 may be a key hydrogen bond to maintain the activity. Notably, the pi-pi

interaction between the lactam ring of compound VS5 and residue His258 does not increase the compound's activity.

All in all, the above five hits, especially compounds VS1 and VS3, can provide references for further design and optimization of ERBB3 inhibitors.

Moreover, various pharmaceutically relevant properties and physical descriptors for ADME properties were also analyzed. As shown in Table 2, all compounds showed ADME parameters within reference range. In silico toxicity risk was also performed to check AMES toxicity, carcinogens, acute oral toxicity, skin permeability, and hepatotoxicity. The compounds are found to have good safety, except five compounds (VS1, VS2, VS3, VS4, and VS5) are predicted as positive for hepatotoxicity. The future work of structure optimization will not only focus on increasing the activities, but also eliminating the toxicities.

## Conclusions

In conclusion, ERBB3 is an important transmembrane receptor and is involved in the intracellular signal transduction network. It is well documented that ERBB3 activation induces the downstream PI3K-AKT and MAPK signaling pathways. This study identified five compounds from natural products database (NPD) and traditional Chinese medicines compounds database (TCMCD) as potential therapeutic agents for the treatment of NSCLC by structure-based virtual screening. In silico ADMET properties filtering was used after docking, but several calculated properties (AlogP, rotatable

**Table 2** Results of in silico prediction of ADMET properties

ADMET properties	VS1	VS2	VS3	VS4	VS5	VS6
BBB	BBB-	BBB-	BBB+	BBB+	BBB+	BBB-
HIA	HIA+	HIA+	HIA+	HIA+	HIA+	HIA+
Pgp substrate	Substrate	Non-substrate	Substrate	Substrate	Substrate	Substrate
VDss (human)	-0.304	-0.864	-0.055	-0.143	-0.812	-0.537
Total clearance	0.839	0.089	0.895	0.129	0.384	0.092
hERG inhibition	Inhibitor	Non-inhibitor	Non-inhibitor	Inhibitor	Inhibitor	Non-inhibitor
AMES toxicity	Non AMES toxic					
Carcinogens	Non-carcinogens	Non-carcinogens	Non-carcinogens	Non-carcinogens	Non-carcinogens	Non-carcinogens
Acute oral toxicity	III	III	III	III	III	III
Skin permeability	No	No	No	No	No	No
Hepatotoxicity	Yes	Yes	Yes	Yes	Yes	No
Molecular weight	534.572	466.497	476.536	585.814	465.513	418.445
LogP	3.41522	5.64994	3.64402	7.1732	3.3033	5.4551
Rotatable bonds	3	7	3	7	5	1
H Bond acceptors	6	5	4	7	6	6
H Bond donors	3	4	3	1	1	2
Surface area	228.999	200.153	207.048	253.486	200.798	178.211

bond, etc.) were considered in the screening process after docking. Availability and prices of compounds were also checked after docking. Compared with the approved drug for lung cancer, nimustine hydrochloride, these five compounds showed relatively good performance. In addition, in silico prediction of ADMET properties indicated that the compounds have good pharmaceutically relevant properties. Because the virtual screening is targeting a new active site, there's no existing experimental models as reference, the preliminary results may have both activity and toxicity.

## Next steps

The hits discovered in this work will provide novel scaffolds for further hit-to-lead optimization and lay the foundation for further development of the therapeutic candidates for NSCLC treatments. The following experiments will focus on structural optimization of these VS-molecules, especially compound VS1, and the proposed binding model still needs more experimental verification. As the inhibitory rates are not very high, structural optimization is needed to find compounds having better inhibitory based on the known structures. On the other hand, we are interested in exploring whether the activity is still maintained *in vivo*, and different xenograft models will be established for the tests.

**Acknowledgments** This work was supported by 2015 prior sci-tech programs of Chinese overseas talents in Beijing, and Beijing Computing Center.

## Reference

- Gridelli C, Perrone F, Monfardini S (1997) Lung cancer in the elderly. *Eur J Cancer* 33(14):2313–2314
- Siegel R, Ma J, Zou Z, Jemal A (2014) Cancer statistics, 2014. *CA Cancer J Clin* 64(1):9–29. doi:[10.3322/caac.21208](https://doi.org/10.3322/caac.21208)
- da Cunha Santos G, Shepherd FA, Tsao MS (2011) EGFR mutations and lung cancer. *Annu Rev Pathol: Mech Dis* 6:49–69
- Dahabreh IJ, Linardou H, Siannis F, Kosmidis P, Bafaloukos D, Murray S (2010) Somatic EGFR mutation and gene copy gain as predictive biomarkers for response to tyrosine kinase inhibitors in non-small cell lung cancer. *Clin Cancer Res* 16(1):291–303. doi:[10.1158/1078-0432.CCR-09-1660](https://doi.org/10.1158/1078-0432.CCR-09-1660)
- Downward J, Yarden Y, Mayes E, Scrace G, Totty N, Stockwell P, Waterfield MD (1984) Close similarity of epidermal growth factor receptor and v-erb-B oncogene protein sequences. *Nature* 307(5951):521–527
- Schechter AL, Stern DF, Vaidyanathan L, Decker SJ, Drebin JA, Greene MI, Weinberg RA (1984) The neu oncogene: an erb-B-related gene encoding a 185,000-Mr tumour antigen. *Nature* 312(5994):513–516
- Kraus MH, Issing W, Miki T, Popescu NC, Aaronson SA (1989) Isolation and characterization of ERBB3, a third member of the ERBB/epidermal growth factor receptor family: evidence for overexpression in a subset of human mammary tumors. *Proc Natl Acad Sci U S A* 86(23):9193–9197
- Plowman GD, Culouscou JM, Whitney GS, Green JM, Carlton GW, Foy L, Shoyab M (1993) Ligand-specific activation of HER4/p180erbB4, a fourth member of the epidermal growth factor receptor family. *Proc Natl Acad Sci U S A* 90(5):1746–1750
- Liu P, Cleveland TE, Bouyain S, Byrne PO, Longo PA, Leahy DJ (2012) A single ligand is sufficient to activate EGFR dimers. *Proc Natl Acad Sci* 109(27):10861–10866
- Cho H, Leahy D (2002) Structure of the extracellular region of HER3 reveals an interdomain tether. *Science* 297(5585):1330–1333
- Falls DL (2003) Neuregulins: functions, forms, and signaling strategies. *Exp Cell Res* 284(1):14–30
- Nakaoku T, Tsuta K, Ichikawa H, Shiraishi K, Sakamoto H, Enari M, Kohno T (2014) Druggable oncogene fusions in invasive mucinous lung adenocarcinoma. *Clin Cancer Res* 20(12):3087–3093. doi:[10.1158/1078-0432.CCR-14-0107](https://doi.org/10.1158/1078-0432.CCR-14-0107)
- Fernandez-Cuesta L, Plenker D, Osada H, Sun R, Menon R, Leenders F, Thomas RK (2014) CD74-NRG1 fusions in lung adenocarcinoma. *Cancer Discov* 4(4):415–422. doi:[10.1158/2159-8290.CD-13-0633](https://doi.org/10.1158/2159-8290.CD-13-0633)
- Salomon DS, Brandt R, Ciardiello F, Normanno N (1995) Epidermal growth factor-related peptides and their receptors in human malignancies. *Crit Rev Oncol Hematol* 19(3):183–232
- Arteaga CL, Engelmann JA (2014) ERBB receptors: from oncogene discovery to basic science to mechanism-based cancer therapeutics. *Cancer Cell* 25(3):282–303. doi:[10.1016/j.ccr.2014.02.025](https://doi.org/10.1016/j.ccr.2014.02.025)
- Schoeberl B, Pace EA, Fitzgerald JB et al (2009) Therapeutically targeting ErbB3: a key node in ligand-induced activation of the ErbB receptor-PI3K axis. *Sci Signal* 2(77):ra31
- Garrett JT, Sutton CR, Kurupi R, Bialucha CU, Ettenberg SA, Collins SD, Arteaga CL (2013) Combination of antibody that inhibits ligand-independent HER3 dimerization and a p110α inhibitor potently blocks PI3K signaling and growth of HER2+ breast cancers. *Cancer Res* 73(19):6013–6023
- Fitzgerald JB, Johnson BW, Baum J, Adams S, Iadevaia S, Tang J, Lugovskoy AA (2014) MM-141, an IGF-IR-and ErbB3-directed bispecific antibody, overcomes network adaptations that limit activity of IGF-IR inhibitors. *Mol Cancer Ther* 13(2):410–425
- McDonagh CF, Huhalov A, Harms BD, Adams S, Paragas V, Oyama S, Nielsen UB (2012) Antitumor activity of a novel bispecific antibody that targets the ErbB2/ErbB3 oncogenic unit and inhibits heregulin-induced activation of ErbB3. *Mol Cancer Ther* 11(3):582–593
- Li D, Ambrogio L, Shimamura T, Kubo S, Takahashi M, Chiriac LR, Wong A (2008) BIBW2992, an irreversible EGFR/HER2 inhibitor highly effective in preclinical lung cancer models. *Oncogene* 27(34):4702–4711
- Patridge E, Gareiss P, Kinch MS, Hoyer D (2015) An analysis of FDA-approved drugs: natural products and their derivatives. *Drug Discov Today* 21:204–207
- Tang JL, Liu BY, Ma KW (2008) Traditional Chinese medicine. *Lancet* 372(9654):1938–1940
- Clardy J, Walsh C (2004) Lessons from natural molecules. *Nature* 432:829–837
- O'Boyle NM, Banck M, James CA, Morley C, Vandermeersch T, Hutchison GR (2011) Open babel: an open chemical toolbox. *J Cheminf* 3:33. doi:[10.1186/1758-2946-3-33](https://doi.org/10.1186/1758-2946-3-33)
- Xinrui S, Da L, Jie C, Yong Z (2014) Computer aided drug screening platform and its application. *Chinese J Bioinform* 12(4)
- Trott O, Olson AJ (2010) AutoDock Vina: improving the speed and accuracy of docking with a new scoring function, efficient optimization, and multithreading. *J Comput Chem* 31(2):455–461
- Cheng F, Li W, Zhou Y, Shen J, Wu Z, Liu G, Lee PW, Tang Y (2012) admetSAR: a comprehensive source and free tool for evaluating chemical ADMET properties. *J Chem Inf Model* 52(11):3099–3105

28. Pires DEV, Blundell TL, Ascher DB (2015) pkCSM: predicting small-molecule pharmacokinetic and toxicity properties using graph-based signatures. *J Med Chem* 58(9):4066–4072
29. Cheng F, Li W, Zhou Y, Li J, Shen J, Lees PW, Tang Y (2013) Prediction of human genes and diseases targeted by xenobiotics using predictive toxicogenomic-derived models (PTDMs). *Mol BioSyst* 9:1316–1325
30. Law V, Knox C, Djoumbou Y, Jewison T, Guo AC, Liu Y, Maciejewski A, Arndt D, Wilson M, Neveu V, Tang A, Gabriel G, Ly C, Adamjee S, Dame ZT, Han B, Zhou Y, Wishart DS (2014) DrugBank 4.0: shedding new light on drug metabolism. *Nucleic Acids Res* 42(D1):D1091–D1097
31. Tosh DK, Padia J, Salvemini D, Jacobson KA (2015) Efficient, large-scale synthesis and preclinical studies of MRS5698, a highly selective A3 adenosine receptor agonist that protects against chronic neuropathic pain. *Purinergic Signal* 11(3):371–387
32. Tominaga H, Ishiyama M, Ohseto F, Sasamoto K, Hamamoto T, Suzuki K, Watanabe M (1999) A water-soluble tetrazolium salt useful for colorimetric cell viability assay. *Anal Commun* 36(2):47–50
33. Miyamoto T, Min W, Lillehoj HS (2002) Lymphocyte proliferation response during *Eimeria tenella* infection assessed by a new, reliable, nonradioactive colorimetric assay. *Avian Dis* 46(1):10–16
34. Weisel M, Proschak E, Schneider G (2007) PocketPicker: analysis of ligand binding-sites with shape descriptors. *Chem Cent J* 1:7
35. Garner AP, Bialucha CU, Sprague ER, Garrett JT, Sheng Q, Li S, Ettenberg SA (2013) An antibody that locks HER3 in the inactive conformation inhibits tumor growth driven by HER2 or neuregulin. *Cancer Res* 73(19):6024–6035
36. Beijing Computing Center—the Department of Computational Medicine—Computer aided drug screening platform (n.d.). Retrieved from <http://www.vslead.com/>
37. Mitsuhashi Y, Lnaba M, Sugiyama Y, Kohayashi T (1992) In vitro measurement of chemosensitivity of human small cell lung and gastric cancer cell lines toward cell cycle phase-nonspecific agents under the clinically equivalent area under the curve. *Cancer* 70(10):2540–2546
38. Saijo N, Niitani H (1980) Experimental and clinical effect of ACNU in Japan with emphasis on small-cell carcinoma of the lung. *Cancer Chemother Pharmacol* 4:165–171